Paper Substrate Spread Function and the MTF of Photographic Paper

Peter G. Engeldrum❖

Imcotek, Winchester, MA, USA

Although the effect of light diffusion in paper on halftone reproduction, as captured in the optical point spread function or its Fourier Transform (MTF), has been known for about half a century, that effect on the microstructure of an image on photographic printing paper in particular, has not been widely studied. The purpose of this work is to construct a simple MTF model of photographic printing paper that specifically includes the effect of the optical MTF of the paper itself and the photographic layer MTF. The MTF for the paper substrate influences the overall MTF at two different stages in the process of exposing and measuring the print MTF. The first influence is during the exposing stage, where the paper substrate MTF acts in a linear manner. In the second, or measurement stage, the process is nonlinear. Because of this nonlinear stage, a Contrast Transfer Function (CTF) descriptor of model component parameters is developed. Model predictions show that it is the paper substrate MTF that dominates the normalized CTF of the resulting photographic print, and not the MTF of the photographic emulsion forming the image. Results from the model are compared with published data, and show good agreement.

Journal of Imaging Science and Technology 48: 50–57 (2004)

Introduction

Although photographic papers have been manufactured for at least as long as film has been made, there is little in the literature on their image microstructure properties. One of the earliest comprehensive experimental investigations of the “sharpness” (really the MTF) of photographic papers is that reported by Ruth Stapleton.[1] One of the general conclusions of her work was that the Modulation Transfer Functions of photographic paper, as measured by edge-gradient analysis, were never as high as those produced by the photographic emulsion (film) by itself. The cited cause of this was the “multiple internal reflexions in the gelatine layer.” Although this is, perhaps, a contributing factor, it does not appear to be the one of consequence. Present knowledge suggests that the most significant factor is the spread of light within the paper base, which we now term the paper optical spread function, POSF, or its Fourier Transform, the paper optical MTF.

The problem of light spreading within the bulk of a paper image substrate was identified by Yule and Nielsen[2] over 50 years ago. Their interest was to explain why the reflectance density of halftone images was higher than that predicted by the ink fractional area of the halftone. They termed this phenomenon “optical dot gain” referring to the apparent increase in dot area due to the paper. Much has been reported in the literature on the topic of dot gain and the spread or diffusion of light in paper. The effort has centered on predicting the mean spectral reflectance or colorimetric values of halftone patterns[2–15] and estimating or measuring the paper optical spread function or its Fourier transform.[4,16–22] Generally speaking, there has been little work done on examining the effect of the POSF, or the paper MTF, on the microstructure of images, but there are some exceptions.[1,23] So far as this author can determine, Stapleton’s report[1] is the only work directed towards photographic printing paper.

The exposing and measurement process of sinusoidal images on photographic *paper* is far more complex than its photographic *film* counterpart. The roots of this complexity can be traced to the paper optical spread function. The POSF contributes to image degradation at both the exposure and measurement or viewing stages. What’s more, at the measurement stage, the system is inherently nonlinear.

The goal of this investigation is to formulate a simple MTF model of a photographic printing paper that includes the MTFs of both the photographic emulsion layer and the paper itself. What is presented in this article is a “small-signal” model of the exposing and measurement of sinusoidal exposure distributions of photographic paper.

Modulation Transfer Function Models

Measuring the MTF of photographic paper is divided into two steps: 1) exposure, and, 2) measurement. In this section, a model for step each is developed.

Exposure MTF Model

The schematic shown in Fig. 1 illustrates the basic construction of a photographic paper. Typically, a coat-

Original manuscript received February 10, 2003

❖ IS&T Fellow

Supplemental Materials—An Appendix can be found on the IS&T website (www.imaging.org) for a period of no less than two years from the date of publication.

pge@imcotek.com

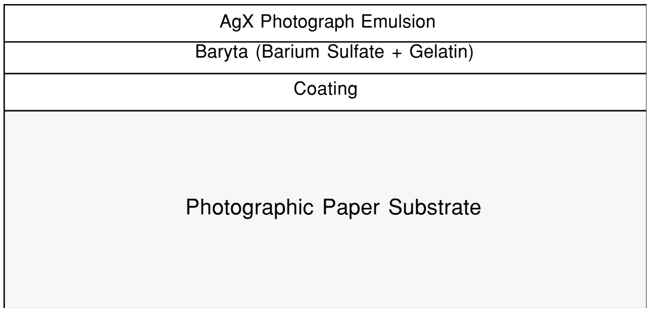

Figure 1. Schematic of the construction of photographic paper.

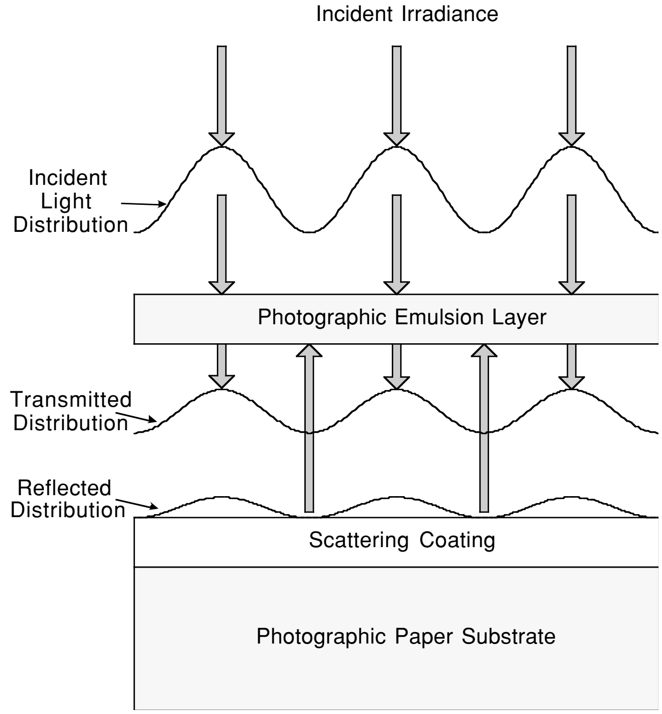

Figure 2. Light flux diagram during the exposing of a photographic paper.

ing of silver halide (AgX) emulsion is applied to a substrate consisting of a high quality coated paper or polymer stock. Beneath the AgX coating is a coated layer of baryta that includes high paper "brightness" and high light scattering among its properties. The coatings contribute to light scattering, as does the substrate itself.

A schematic of the exposing process is illustrated in Fig. 2. The exposure consists of a one-dimensional normally incident sinusoidal relative intensity distribution described by Eq. (1).

$$i_0(x) = \bar{I}\left[1 + M_e \cos(2\pi u_0 x)\right] \tag{1}$$

where I is the average irradiance, M_e is the sinusoidal exposure modulation, = (max – min)/(max + min), x is distance, mm, and u_0 is the spatial frequency, cycles/mm, of the sinusoidal exposure. For simplicity, only the relative intensity is considered in this model. Exposure is given by suitable multiplicative scaling constants. In practice, the model parameters are all functions of wavelength, λ. Wavelength notation is not explicitly carried in the model, but should be in some situations.

During the initial exposure, the light incident on the AgX layer is channeled three ways: the AgX coating (emulsion) absorbs some of the light, a_e, some is transmitted, t_e, and some is reflected by the emulsion surface. The reflected component is ignored in this model because it is assumed not to contribute to the exposure. The sinusoidal light distribution entering the photographic layer is assumed to be scattered by the emulsion coating as it passes through the layer. This scattering is represented by the well-known modulation transfer function of the film, $T_f(u_0)$, for both the absorbed light, exposure, and the transmitted light. A fraction of this scattered light that is equal to the AgX layer absorptance, a_e, is assumed to be proportional to the exposure. Thus, the exposure for the first pass of the light through the photographic emulsion is given by Eq. (2).

$$H_I(x) = a_e\bar{I}\left[1 + T_f(u_0)M_e \cos(2\pi u_0 x)\right] \tag{2}$$

The spatial distribution of the light after passing through the emulsion layer and before encountering the paper substrate is proportional to the light transmitted by the AgX layer, and is given by Eq. (3).

$$i_t(x) = t_e\bar{I}\left[1 + T_f(u_0)M_e \cos(2\pi u_0 x)\right] \tag{3}$$

At this point, the sinusoidal light distribution at spatial frequency u_0 has been reduced in modulation by the modulation transfer factor, $T_f(u_0)$, of the AgX layer. This transmitted sinusoidal light pattern is then incident on the paper substrate. The overall amount of reflected light is reduced by the paper reflectance factor, r_p. The modulation of the reflected sinusoidal light distribution is reduced by the paper MTF, $T_p(u_0)$. This assumes that the diffusion of light within the paper is linear with no phase shifts. For this linear case the reflected sinusoid is just reduced in modulation by the paper MTF.[6] Although this assumption does not seem to have been explicitly tested, the measured data to date[21] suggests that the assumption is quite reasonable. Thus, the reflected light distribution at the surface of the paper substrate is given by Eq. (4).

$$i_r(x) = r_p t_e\bar{I}\left[1 + T_f(u_0)T_p(u_0)M_e\cos(2\pi u_0 x)\right] \tag{4}$$

The light that is coming from the direction of the paper substrate, reflected light, constitutes a second exposure to the AgX layer. Assuming, again, that the absorbed fraction is proportional to the exposure, the second relative exposure distribution is given by Eq. (5). Note that the AgX layer MTF enters twice, once for each direction the light is propagating, and thus is a squared quantity.

$$H_{II}(x) = a_e r_p t_e\bar{I}\left[1 + T^2{}_f(u_0)T_p(u_0)M_e \cos(2\pi u_0 x)\right] \tag{5}$$

If we now simply assume that the two exposure distributions $H_I(x)$ and $H_{II}(x)$ add, then the total relative exposure distribution for the photographic layer is just the sum of the two exposure distributions in each direction, Eqs. (2) and (5). This is given by Eq. (6), with scaling constants omitted.

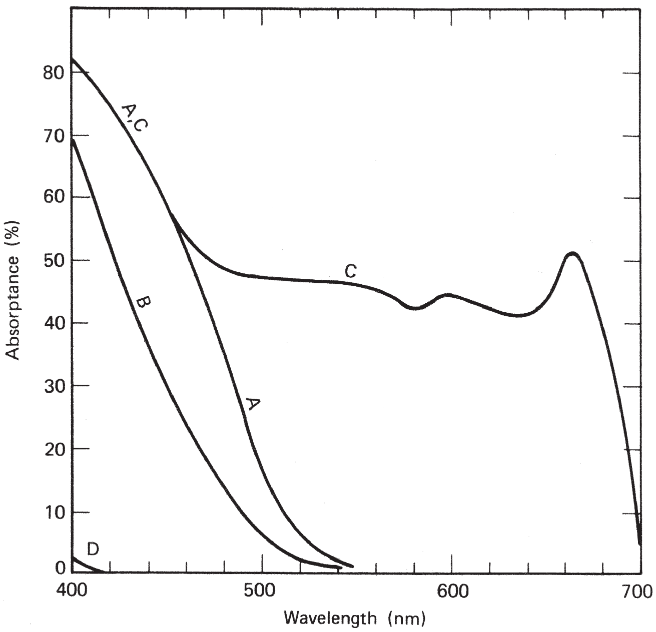

Figure 3. Spectral absorptance for several silver halide emulsions. A = undyed negative type; B = extremely fined grain; C = same as A with a spectral sensitizing dye; and D = pure silver chloride (from Ref. 27).

$$H_T(x) = \left\{1 + r_p t_e + M_e T_f(u_0)\cos(2\pi u_0 x)\left[1 + r_p t_e T_f(u_0) T_p(u_0)\right]\right\} \quad (6)$$

The exposure modulation is computed by taking the difference between the maximum and minimum exposures and dividing that by the sum of the maximum and minimum. Since we assume the scattering is isotropic, there is no reason to assume any spatial phase shifts of the exposure distribution. Without spatial phase shifts, the maximum occurs at $x = 0$ and the minimum at $x = 1/2\ u_0$. Dividing the exposure modulation by the input modulation, M_e, yields the exposure MTF, $T_{fe}(u)$, of the photographic paper. The exposure MTF incorporates the paper substrate MTF, the emulsion layer MTF, the reflectance of the paper, and the transmittance of the AgX layer. Equation (7) shows this result.

$$T_{fe}(u) = \frac{T_f(u)\left[1 + r_p t_e T_f(u) T_p(u)\right]}{1 + r_p t_e} \quad (7)$$

This equation reveals that the exposure MTF of the photographic paper is not simply the MTF of the emulsion layer, $T_f(u_0)$. The "intrinsic" MTF of the AgX layer is reduced by a function that depends on the transmittance of the emulsion layer, the reflectance of the paper, and the paper MTF. For very low spatial frequencies, the exposure MTF is approximately equal to the MTF of the AgX layer. At spatial frequencies where the paper MTF is zero, the exposure MTF is the AgX emulsion layer MTF reduced by a factor equal to $1/(1 + r_p t_e)$. Since this factor lies in the interval between one and two, inherent emulsion MTF is reduced by a factor of two at most.

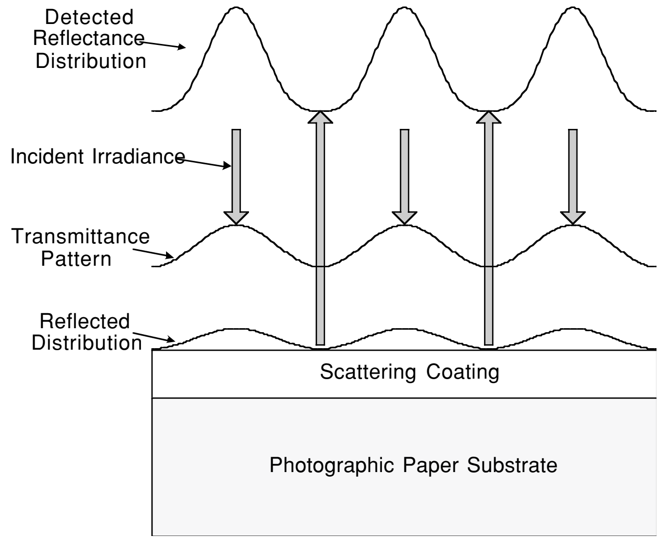

Figure 4. Light flux diagram for sinusoidal layer on paper.

Note that since $T_f(u_o)$ and $T_p(u_0)$ are typically less than unity, the photographic paper exposure MTF is always less than the AgX emulsion layer alone. From a photographic print paper design point of view, the exposure MTF can be maximized by reducing either the paper reflectance, the emulsion transmittance, or both. Reducing the paper reflectance substantially will reduce the paper lightness/brightness, and therefore is not practical. Thus, varying the emulsion transmittance is the only model variable available. Figure 3 shows percent absorptance versus wavelength for some representative silver halide emulsions.[27] Note that these spectral absorptance curves are strong functions of wavelength. Reducing the emulsion transmittance by incorporating a dye is a well-known tactic for increasing spectral sensitivity and improving the spatial frequency response by reducing halation in photographic films.[24b] However, there seems to be little in the literature regarding usage of dye in photographic papers to control the MTF.

AgX Layer Sensitometric Assumptions

The latent, or exposure, image is inaccessible to measurement before the conversion to a silver image via development. Common practice for determining the MTF of photographic materials is to incorporate various levels of exposure in the form of large-area gray patches. These patches serve to characterize the nonlinear emulsion (film) response to light, via a density versus log exposure, log (H), or other suitable calibration curve. The purpose of this calibration curve is to determine the effective exposure of the sinusoidal patterns.[24a] To avoid this model complexity, an approximation can be developed by assuming a small modulation sinusoidal pattern.

The transmittance image distribution, for a D–log(H) curve of instantaneous slope, γ, is given by Eq. (8).[24a]

$$t(x) = kH(x)^{-\gamma} \quad (8)$$

In order to develop a closed form solution, and in the interest of simplicity, the small modulation approximation for the developed sinusoidal transmittance image is used, which is given by Eq. (9). This equation can be developed by substituting Eq. (1) into Eq. (8) and using the first term of the binomial expansion.

$$t_I(x) = \left(\bar{I}\right)^{-\gamma}\left[1 - \gamma T_f(u_0) M_e \cos(2\pi u_0 x)\right] \tag{9}$$

This equation is a good approximation for modulations $M < 0.15$ and $n < 2.5$. For parameters within these ranges, the relative amplitude of the second harmonic is typically < 0.01 and the transmittance image is practically a pure sinusoid.

Measurement MTF Model

The measurement or viewing of an image on a photographic paper or other scattering substrate is schematically illustrated in Fig. 4. Once the exposed photographic paper is developed, a low modulation sinusoidal transmittance image exists on the paper substrate, as defined by the following, Eq. (10).

$$t_I(x) = \bar{t}\left[1 - M_i \cos(2\pi u_0 x)\right] \tag{10}$$

where t = the average transmittance of the sinusoidal target and M_i = modulation of the sinusoidal transmittance image in contact with the paper substrate. Note that $M_i = \gamma\ T_{fe}(u) M_e$ using the small modulation approximation.

The measurement model assumes the same layered structure as the exposure model, with the exception that the illumination intensity is spatially uniform and is modulated by the transmittance image in the photographic emulsion layer. The sinusoidal intensity distribution is reduced in modulation by the same paper spread function (MTF) that reduced the modulation of the exposure image. Again, as in the exposure step it is assumed that diffusion is a linear process. The reflected light must now pass back through the sinusoidal transmittance image before the measuring instrument can detect it. This multiplication step gives rise to a nonlinear system that generates a frequency of twice the frequency of the sinusoidal transmittance distribution. This reflected light distribution is described by Eq. (11).

$$R(x) = \bar{t}^2 r_p \begin{bmatrix} 1 + \dfrac{M_i^2 T_p(u_0)}{2} - \left\{1 + T_p(u_0)\right\} M_i \cos(2\pi u_0 x) \\ + \dfrac{M_i^2 T_p(u_0)}{2} \cos(2\pi 2 u_0 x) \end{bmatrix} \tag{11}$$

Finally, since the measurement instrument does not have perfect spatial frequency response, the detected sinusoidal image is reduced in modulation by the MTF of the measuring instrument according to Eq. (12).

$$R(x) = \bar{t}^2 r_p \begin{bmatrix} 1 + \dfrac{M_i^2 T_p(u_0) T_m(u_0)}{2} - \left\{1 + T_p(u_0)\right\} T_m(u_0) M_i \cos(2\pi u_0 x) \\ + \dfrac{M_i^2 T_p(u_0) T_m(2u_0)}{2} \cos(2\pi 2 u_0 x) \end{bmatrix} \tag{12}$$

Since the measurement process is inherently nonlinear, it is not strictly correct to formulate a linear system modulation transfer function from Eq. (12). Instead, a Contrast Transfer Function, *CTF*, is defined via the minimum and maximum of the sinusoidal reflectance distribution described by Eq. (12). This *CTF* is defined by Eq. (13), which is more comprehensive than previously reported results.[22]

$$CTF(u) = \frac{M_i T_m(u)\left[1 + T_p(u)\right]}{1 + \dfrac{M_i^2 T_m(u) T_p(u)}{2}\left[1 + \dfrac{T_m(2u)}{T_m(u)}\right]} \tag{13}$$

If the spatial frequencies are low enough, or the measurement instrument has sufficiently high MTF, then the ratio of the two MTFs in the denominator of Eq. (13) is approximately 1.0 and we can rewrite Eq. (13) in a simpler form as Eq. (14).

$$CTF(u) = \frac{M_i T_m(u)\left[1 + T_p(u)\right]}{1 + M_i^2 T_m(u) T_p(u)} \tag{14}$$

Careful perusal of Eq. (14) will reveal that there is a low spatial frequency "gain" factor associated with the transmittance image on paper. For low modulations, M_i, $CTF(0)$ approaches $2M_i$, but as M_i approaches 1.0, $CTF(0)$ approa2ches M_i. Thus, there is an interesting low-contrast gain factor, with a maximum value of 2, that enhances the contrast (modulation) of low-contrast imagery. Note also that as the spatial frequency increases and $T_p(u)$ approaches zero, the *CTF* approaches the limiting value of M_I; i.e. $CTF(\infty) \rightarrow M_i$.

If one assumes that the measurement instrument has a high MTF, ≈ 1.0, compared to the optical MTF of the paper, and uses low-modulation sinusoids, then Eq. (14) can be further simplified to yield a simple equation for the paper MTF. Note that the denominator in Eq. (14) is at most $1 + M_i^2$. Further, when using small M_i, the denominator of Eq. (14) is approximately 1.0, independent of spatial frequency. These assumptions yield the approximation given in Eq. (15).

$$CTF(u) \approx M_i\left[1 + T_p(u)\right] \tag{15}$$

Solving Eq. (15) for the paper MTF, $T_p(u)$, yields Eq. (16), which can be used as an estimator for the paper MTF.

$$T_p(u) \approx \left[\frac{CTF(u)}{M_i} - 1\right] \tag{16}$$

The two variables in Eq. (16)–the modulation of the sinusoidal transmittance image, M_i, and the measured contrast transfer function, $CTF(u)$—are either known or readily measured, and thus Eq. (16) can be used to estimate the paper MTF. It is important to emphasize that Eq. (16) is valid only for the case of low modulations, and with no modulation reduction due to the measuring instrument. In other cases, Eq. (14) should be used to solve for $T_p(u)$ via numerical methods.

Complete *CTF* Model

Equation (17) shows the complete relationship for the overall *CTF* model for photographic printing paper combining the exposure MTF and measurement *CTF*, including the measurement-device MTF.

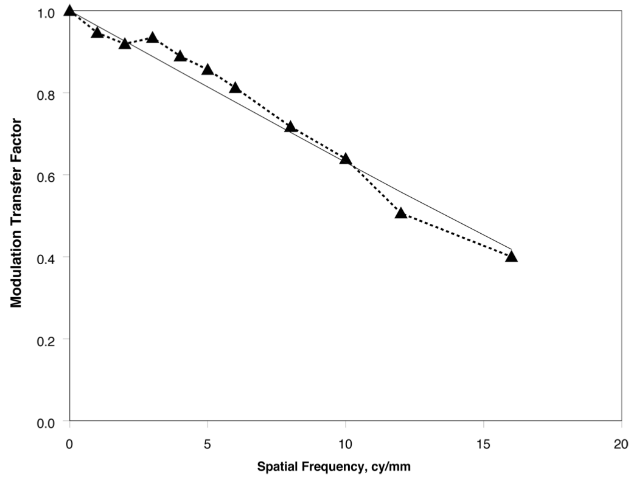

Figure 5. Comparison of measured MTF of Microtek Scanmaker 5 desktop scanner, triangles, and diffraction limited lens least squares fit, solid line.

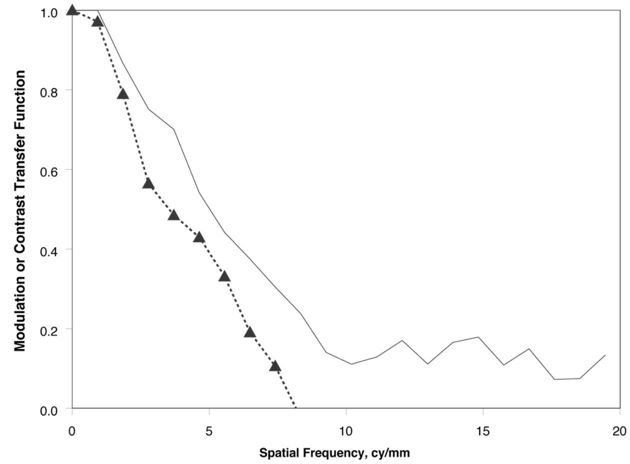

Figure 6. Comparison of paper MTF measurements using contact sinusoids, triangles, and a measurement using Edge Gradient Analysis, solid line.

$$CTF(u) = \frac{\dfrac{\gamma M_e T_f(u) T_m(u)}{1 + r_p t_e}\left[1 + r_p t_e T_f(u) T_p(u)\right]\left[1 + T_p(u)\right]}{1 + \dfrac{1}{2}\left\{\dfrac{\gamma M_e T_f(u)}{1 + r_p t_e}\left[1 + r_p t_e T_f(u) T_p(u)\right]\right\}^2 T_p(u) T_m(u)\left[1 + \dfrac{T_m(2u)}{T_m(u)}\right]} \tag{17}$$

Experiments

Comparison of the *CTF* or MTF model for photographic printing paper is made difficult by the dearth of data in the literature. However, two experiments are described supporting the validity of the model components. The first compares the MTF of paper via the measurement model of Eq. (14), with reported results using edge gradient methods. The second experiment fits the overall model of Eq. (17) to data reported in Ref. (1).

Measurement Model Feasibility Test

The feasibility of the measurement model was tested using the contact method[22] with a transmittance sinusoidal pattern, model M-14-80 from Sine Patterns.[25] This pattern was put in contact with a matte-coated ink jet paper whose MTF had been previously measured via the edge gradient technique.[18] This sandwich was placed with the transmittance sinusoidal pattern and a calibrated reflectance gray scale on the platen glass of a Microtek Scanmaker 5 desktop scanner and scans were made at 1000 samples/inch.

The MTF of the Scanmaker 5 was measured using a model M-15-60 sinusoidal reflectance pattern, also from Sine Patterns. The maximum and minimum reflectances of the sinusoids were estimated from gray level histograms of the patterns using the most frequently occurring values. These minimum and maximum reflectance values were converted to min and max reflectance via a digital-value-versus-reflectance calibration curve that was generated from the calibrated reflectance gray scale.

Since the transparency is not in intimate contact with the paper substrate, this sandwich of transparency and paper is not optically the same as photographic paper. But one might nonetheless expect reasonable "order of magnitude" results. In this case, the objective was to obtain an estimate for the known paper MTF, which can be estimated from a modified from of Eq. (14). Equation (14) was modified by keeping the MTF of the measurement device–the scanner–only in the numerator of the equation.

Equation (14) is quite simple, but in practice the computed values have high variance due to the high error (noise) in all the measured quantities. In fact, to make use of this equation, some data "smoothing" must be used. Data smoothing in this case consisted of fitting simple functions to the measured data via least squares techniques.

For the MTF of the scanner, the measured sine wave data was fit to the MTF of a diffraction-limited clear circular lens using the Hufnagle polynomial approximation,[26] given in Eq. (18).

$$T_{lens}(u) = 1 - 1.25(uf\lambda) + 0.25(uf\lambda)^4 \tag{18}$$

The f/number, f, was $f/54$, assuming a median wavelength, λ, of 500 nm The RMS error about the curve, determined via least squares fit, was 0.035. The measured scanner MTF data and the plot of Eq. (18) using these parameter values is shown in Fig. 5.

Figure 6 shows a comparison of the paper spread function estimated using the contact sinewave method and the edge gradient method.[18] The estimate of the paper MTF shown here is an improved version of that reported in Ref. 18. The improvement consists of median filtering the edge before the numerical differentiation. Agreement between the two methods is quite good considering the many assumptions, the potential for interfacial re-

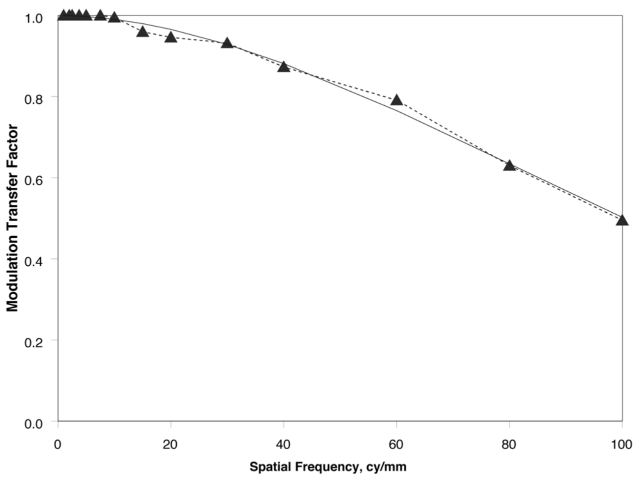

Figure 7. Comparison of measured film MTF, triangles, and exponential film model least squares fit, solid line. Measured film MTF data from Ref. 1.

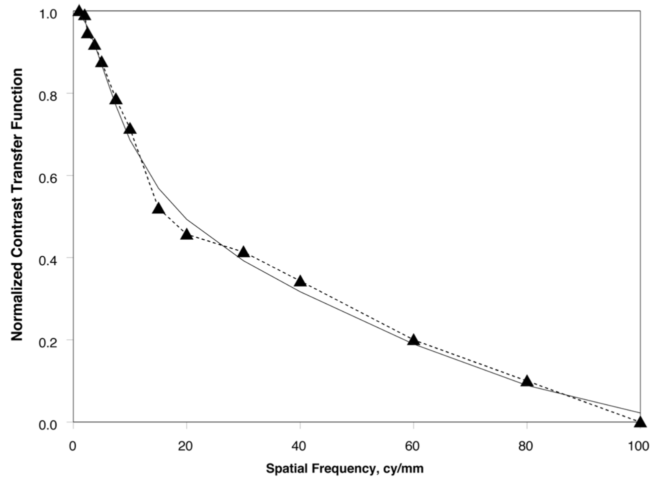

Figure 8. Comparison of the complete model given by Eq. (17), solid line, and measured data from Ref. (1), triangles. See text for model parameter values.

flections between paper-sine wave pattern, and differences in illumination geometry.

These results are quite encouraging and suggest that the measurement model is at least reasonable. However, the fluctuations of real measurements are too high to compute the paper MTF by frequency-by-frequency application of Eq. (16). Additional work is needed on a statistical estimator for the paper MTF, via Eq. (13) or its modification, before this can be considered a routine practical method.

Model-Data Comparison

The second experiment consisted of a comparison of the photographic paper contrast transfer function model to published data. This presented a significant challenge because the key model parameters are not generally known.

The strategy was to use data published by Stapleton,[1] fix a small number of parameters, and estimate the paper MTF parameters that best fit the data in a least squares sense. It turns out that only one parameter, the AgX layer transmittance, can be arbitrarily fixed. The paper reflectance, assumed to be R_∞ in Kubelka–Munk theory, is a parameter of the paper MTF model[18] so was not independently variable (see Appendix, *available as Supplemental Material on the IS&T website (www.imaging.org) for no less than two years from the date of publication*). For the paper MTF model, Eq. (A3) was used.[18]

Stapleton's film MTF data curve B [Fig. 3 of Ref. 1] was taken as the model value of $T_f(u)$. A least squares fit of the film MTF to an exponential function of the form shown in Eq. (19) was used for the calculations.

$$T_f(u) = \exp(-b\,|\,u\,|^{a}) \qquad (19)$$

The fit to the data yielded the parameter values a = 1.899 and b = 0.0001105, for an RMS error about the fit of 0.012. Figure 7 shows the comparison of the function fit and the data from Ref. (1).

It is not entirely clear from Stapleton's work.[1] whether all the published MTF curves were corrected for the measurement MTF, a 9 μm slit. For this reason, a slit width parameter, w, using the well-known Sinc function, $\sin(\pi uw)/(\pi uw)$ for the measurement MTF, was added to the least squares calculation. Preliminary computations suggested that excellent least squares fits to the measured paper MTF could be obtained by varying R_∞, the scattering coefficient, S, and slit width w. In all these preliminary computations, the slit width parameter estimate was almost constant at 9 mm (± 10%), which suggests that the effect was not removed from the published data.[1]

Considering these preliminary results, the computational strategy was altered to keep a fixed value of R_∞ and solve for S and w. R_∞ was taken to be equal to the paper reflectance in the model calculations. Both S [see Eq. (A3) in the Appendix] and w control the roll-off rate of the measured *CTF* and thus provide *CTF* shaping.

The computational procedure consisted of selecting the two parameters–the emulsion transmittance, t_e, and R_∞– and fitting the model by solving for the paper scattering coefficient, S, Eq. (A3), and slit width, w. The S and w estimates minimized the mean-squared difference between the model *CTF*, Eq. (16), normalized so $CTF(0) = 1$, and the curve C in Stapleton's Fig. 3.[1] This yields a comparison of Stapleton's data with model calculations. The parameters values γ = 1.5 and M_i = 0.15 we kept fixed for all calculations.

Model Results

A number of good fits were obtained over a wide range of S, t_e and R_∞. However, not all of these solutions were particularly realistic. A decision was made to restrict the range of the free parameter R_∞ to the interval of 0.6 to 0.95. This range corresponds to a paper reflection density range of 0.02 to 0.22. Published data for coated non-photographic paper suggested that reasonable values of the scattering coefficient, S, lie in the range from 5 mm^{-1} to 150 mm^{-1}.[18,19] The absorption coefficients, K and S, and R_∞ are locked together. Therefore, given any two, the other can be determined.[28] Given the above range of parameters, K, in mm^{-1}, will lie in the range of 6×10^{-3} to 13.

The transmittance of the photographic paper AgX layer is completely unknown except for the guidance

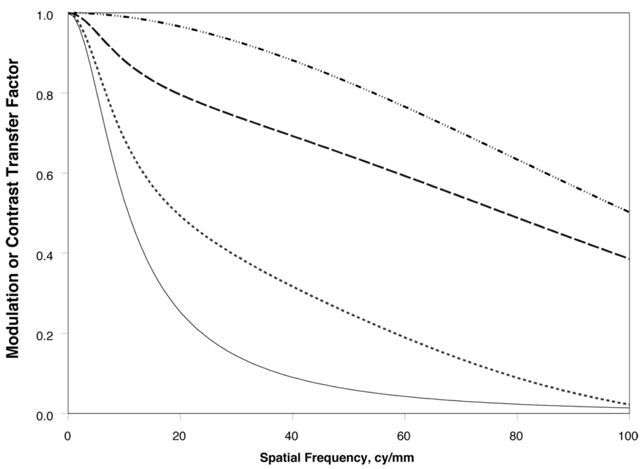

Figure 9. Component model MTF/CTFs. Top curve, dot-dash is the film emulsion MTF, dashed curve is the paper exposure MTF from Eq. (7), dotted curve is model CTF (same as Fig. 8), and the solid curve is the paper substrate MTF using the estimated model parameters.

provided by Fig. 3. Using a fixed emulsion transmittance in the range of 0.1 to 0.5 for each of the least squares fits gave reasonable values of S.

Figure 8 shows the comparison of model results with the measured data for the model parameters values; $R_\infty = 0.80$, $S = 143$ mm^{-1} and $t_e = 0.5$. The RMS error about the fit is 0.024 in CTF units. Figure 9 shows the model component results for this set of parameters. The top curve, dot–dash, is the function fit, Eq. (18) to the measured film MTF from Ref. (1). The next lower curve, dashed, is the exposure MTF from Eq. (7). The third curve from the top, dashed, is the model fit to the data. Finally, the bottom curve is the paper MTF according to Eq. (A3) using the estimated model parameters.

Discussion

The proposed model provides a very good fit to the measured data. In particular, it models the "break point" in the MTF/CTF curves for photographic paper[1] with reasonable parameter values for the paper and AgX layer. Further testing is required to see how robust the model is for a variety of photographic papers.

According to this model, Eq. (7), the recovery of the photographic paper exposure MTF is not simple. It does not appear that the standard practice of dividing the measured MTF/CTF, or SFR, by the input pattern/target modulation is completely adequate to recover the exposure MTF, $T_{fe}(u)$, under all circumstances. Having several unknown quantities complicates the recovery process.

This simple model shows that there are no practical circumstances where the photographic paper MTF/CTF can be equal to the exposure MTF of the silver halide layer. The CTF is typically degraded toward the paper MTF, but remains higher over most of the spatial frequency bandwidth. The inaccessible exposure MTF of the AgX emulsion coating and the MTF of the paper itself give some insight into *why* it is difficult to produce sinusoidal test patterns of high modulation at high spatial frequency using conventional photographic processes.

The model has been developed in the context of a silver halide material as the light-sensitive coating on the paper substrate. However, the model may apply equally well to any other light-sensitive coating, or any imaging system that can sum exposures. The MTF/CTF of any sort of imaging system that has the light detection mechanism before some finite substrate with reflecting and scattering properties should behave similarly.

It is important to note that all of the functions and parameters in the model are wavelength dependent, although not explicitly formulated as such. Photographic emulsion absorptances, and paper scattering and absorptance are generally wavelength dependent. This dependence, particularly in the short wavelengths, is responsible for yellow appearance of papers and photographic emulsions. For color imaging applications, this wavelength dependence can be critically important.

Conclusions

A simple model of the exposing and measuring components of a sinusoidal test pattern exposure of photographic paper has been constructed which can be used to estimate the modulation transfer function, MTF, of a photographic printing paper. Under suitable assumptions, the exposing part is linear, and yields an MTF for exposure. However, the measurement component is nonlinear and is characterized by a contrast transfer function, CTF. Key model parameters include: 1) the light-sensitive coating transmittance, 2) the reflectance factor of the paper substrate, 3) the Kubelka–Munk scattering coefficient of the paper, 4) the reflectivity, R_∞, of the substrate, 5) the photographic layer MTF and 6) the image measurement device MTF.

The measurement model component was tested using a contact sinusoidal pattern to estimate the known MTF of a matte coated ink jet paper. Reasonable agreement was found between the contact method and the edge-gradient method. However, the contact method of paper MTF estimation is quite sensitive to measurement errors.

The complexity of the model has implications for using photographic paper reflectance patterns when testing imaging systems such as desktop scanners. Since the Fourier spectrum of the pattern will be limited by the paper or other scattering substrate, instead of the photographic emulsion itself, it is extremely difficult to fabricate high modulation patterns at high spatial frequencies or "perfect" edges.

Although the model is described in the context of a photographic paper it should also be useful for any imaging system that sums of two spatially or spectrally filtered versions of the same input signal/image.

Appendix

Available as Supplemental Material on the IS&T website (*www.imaging.org*) for no less than two years from the date of publication).

References

1. R. E. Stapleton, The sharpness of reflected images, *J. Photogr. Sci.* **12,** 289 (1964).
2. J. A. C. Yule and J. W. Nielsen, The penetration of light into paper and its effect on halftone reproduction, *Proc. TAGA*, 65 (1951).
3. G. Jorgensen, *Research Progress* **47,** 1 (1960), (Graphic Arts Technical Foundation, Pittsburgh, PA).
4. J. A. C. Yule, D. Howe and J. Altman, The effect of the spread function of paper on halftone reproduction, *TAPPI*, **50,** 337 (1967).
5. H. Wakeshima, T. Kunishi and S. Kaneko, Light scattering in paper and its effect on halftone reproduction, *J. Opt. Soc. Amer.* **58,** 272 (1968).
6. F. R. Ruckdeschel and O. G. Hauser, Yule–Nielsen effect in printing: a physical analysis, *Appl. Optics* **17,** 3376 (1978).
7. P. Engeldrum, The color between the dots, *J. Imaging Sci. Technol.* **23,** 545 (1994).

8. M. Wedin, and Björn Kruse, Halftone colour prints: dot gain and modelling of colour distributions, *Proc. SPIE* **2413,** pp. 344–355 (1995).
9. Björn Kruse and M. Wedin, A new approach to dot gain modeling, *Proc. TAGA*, 329 (1995).
10. S. Gustavson, M. Wedin and B. Kruse, 3D modeling of light diffusion in paper, *Proc. TAGA*, 848 (1995).
11. J. S. Arney, P. G. Engeldrum, and H. Zeng, An expanded Murray–Davies model of tone reproduction in halftone imaging, *J. Imaging Sci. Technol.* **39,** 502 (1995).
12. P. G. Engeldrum The color gamut limits of halftone printing with and without the paper spread function, *J. Imaging Sci. Technol.* **40,** 239 (1996).
13. J. S. Arney, Charles D. Arney and P. G. Engeldrum, Modeling the Yule–Nielsen halftone effect, *J. Imaging Sci. Technol.* **40,** 233 (1996).
14. G. L. Rogers, Optical dot gain in a halftone print, *J. Imaging Sci. Technol.* **41,** 643 (1997).
15. G. L. Rogers, Effect of light scatter on halftone color, *J. Opt. Soc. Amer. A* **17,** 1813 (1998).
16. F. C. Eisen, A reflection micro-scanning instrument, in *Image Analysis and Evaluation*, R. Shaw, Ed., IS&T, Springfield, VA, 1977, p. 12; ISBN 0892080892
17. D. Lehmbeck, and J. J. Jakubowski, Optical principles and practical considerations for reflection microdensitometry, *J. Appl. Photogr. Eng.* **5,** 63 (1979).
18. P. G. Engeldrum and B. J. Pridham, Application of turbid medium theory to paper spread function measurements, *Proc. TAGA*, Vol. I, 339 (1995).
19. J. S. Arney, C. D. Arney, M. Katsube, and P. G. Engeldrum, An MTF analysis of papers, *J. Imaging Sci. Technol.* **40,** 19 (1996).
20. G. L. Rogers, Measurement of the modulation transfer function of paper, Appl. Opt. **37,** 7235 (1997).
21. S. Inoue, N. Tsumura and Y. Miyake, Measuring MTF of paper by sinusoidal test pattern projection, *J. Imaging Sci. Technol.* **41,** 657 (1997).
22. S. Inoue, N. Tsumura and Y. Miyake, Analyzing *CTF* of print by MTF of paper, *J. Imaging Sci. Technol.* **42,** 572 (1998).
23. M. Maltz, Light scattering in xerographic images, *J. Appl. Photogr. Eng.* **9,** 83 (1983).
24 T. H. James, Ed., *The Theory of the Photographic Process*, 4th Ed., Macmillan, New York, NY 1977, chap. 20, 21, and 24b; ISBN 0023601906.
25. Sine Patterns, Pittsford, NY http://www.sinepatterns.com
26. R. E. Hufnagle, Simple approximation to diffraction limited MTF, *Appl. Optics* **10,** 2547 (1971).
27. W. Thomas, Ed., *SPSE Handbook of Photographic Science and Engineering*, John Wiley and Sons, New York, 1973, p 441, ISBN 0471818801.
28. P. Kubelka, New contributions to the optics of intensely light-scattering materials. Part I *J. Opt. Soc. Amer.* **38,** 448 (1948).